ELSEVIER

Physica E 10 (2001) 428–432

PHYSICA E

www.elsevier.nl/locate/physe

MBE growth of ferromagnetic single crystal Heusler alloys on (0 0 1)$Ga_{1-x}In_xAs$

J.W. Dong[a], J. Lu[a], J.Q. Xie[a], L.C. Chen[a], R.D. James[b], S. McKernan[c], C.J. Palmstrøm[a,*]

[a] *Department of Chemical Engineering and Materials Science, University of Minnesota, Minneapolis, MN 55455, USA*
[b] *Department of Aerospace Engineering and Mechanics, University of Minnesota, Minneapolis, MN 55455, USA*
[c] *Center for Interfacial Engineering, University of Minnesota, Minneapolis, MN 55455, USA*

Abstract

Ferromagnetic Ni_2MnGa and Ni_2MnGe have been grown on GaAs(0 0 1) and Ni_2MnIn on InAs(0 0 1) by molecular beam epitaxy. In situ reflection high energy electron diffraction, ex situ X-ray diffraction and transmission electron microscopy selected area electron diffraction indicate the growth of pseudomorphic single crystal (0 0 1) Ni_2MnGa on (0 0 1) GaAs. Superconducting quantum interference device magnetometry measurements show the films to be ferromagnetic with in-plane magnetization and Curie temperatures of ~340, ~320, and ~290 K for Ni_2MnGa, Ni_2MnGe and Ni_2MnIn, repectively.

PACS: 75.70 Ak; 75.50.Cc; 81.15.Hi

Keywords: Heusler alloys; Ni_2MnGa/GaAs; Ni_2MnGe/GaAs; Ni_2MnIn/InAs; MBE

1. Introduction

The recent ability of making ferromagnetic semiconductors [1] and the observation that the spin coherence length can be as large as 100 μm in a semiconductor [2] have stimulated the integration of magnetic materials and semiconductors to make novel devices that utilize the carrier spin as well as its charge [3]. A key element to develop "spintronic" devices is the ability to electrically inject spin polarized carriers into an otherwise unpolarized semiconductor. Recently, two groups have reported the spin polarized injection of electrons from a magnetic semiconductor at low temperature [4,5]. There has been only limited success injecting carriers with large spin polarization into a semiconductor from a ferromagnetic metal contact [6,7]. This is believed to result from poor interface properties, both electrical and magnetic, and from the lack of sufficient spin polarization of the ferromagnet at the Fermi level [8]. For diffusive transport, recent theories suggest that close to 100% spin polarization

* Corresponding author.
E-mail address: palms001@tc.umn.edu (C.J. Palmstrøm).

1386-9477/01/$ - see front matter
PII: S1386-9477(01)00131-X

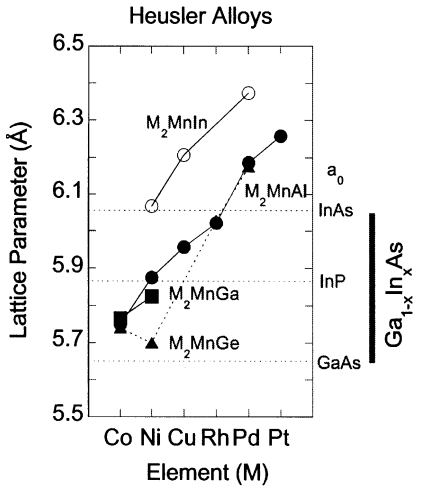

Fig. 1. Lattice parameter versus element for a number of compounds with the Heusler structure.

at the Fermi level (half-metallic ferromagnetism) will be needed for significant spin injection [9]. Although a number of ferromagnetic compounds have been predicted theoretically to be half-metallic, experimentally 100% spin polarization at the Fermi level has not been observed [10]. However, contacts utilizing ballistic transport are more likely to inject high spin polarization [11]. For spin-polarized ballistic transport, matching of the band structure of the ferromagnetic metal and the semiconductor is very important [12,13]. Kilian and Victora [13] predicted that the band structure alignment between the Heusler alloy Ni_2MnIn and InAs would enhance the injection of the minority spins. Their calculations show that the minority spins are situated at the Γ point in Ni_2MnIn and the majority spins are far away from the Γ point. This is what makes the transmission coefficient much larger for the minority than the majority spins, suggesting that Heusler alloys may be a good choice as a ferromagnetic contact for spin injection. Recently the epitaxial growth of Ni_2MnGa [14–16] and Co_2 MnGe [17] on GaAs(0 0 1) have been reported.

Fig. 1 shows a plot of the lattice parameter versus transition element for a number of Heusler alloys with the $L2_1$ crystal structure. The mismatch for Ni_2MnGa, Ni_2MnGe and Co_2MnGe to GaAs are 3%, 0.83% and 1.5%, respectively. Ni_2MnIn is closely lattice matched to InAs (mismatch $\sim$0.16%). In this paper, we report on the amazing compliancy of Ni_2MnGa grown on GaAs(0 0 1), the molecular beam epitaxial (MBE) growth of Ni_2MnGe on GaAs(0 0 1) and Ni_2MnIn on InAs(0 0 1) and their magnetic properties.

2. Experimental

In order to minimize Mn contamination of the compound semiconductor growth chamber, the GaAs and InAs buffer layers were grown in a separate growth chamber from the Heusler alloy growth. GaAs layers were grown on GaAs(0 0 1) substrates at 580°C in a modified VG V80H MBE system. The samples were arsenic capped by allowing the sample to cool overnight facing the liquid nitrogen cryopanel with a chamber pressure $\leqslant 5\times10^{11}$ mbar. The arsenic capping was performed with a sample temperature < -10°C using an As_4-flux. In the case of buffer layers for Ni_2MnGa growth an additional six monolayer thick $Sc_{0.3}Er_{0.7}As$ was grown at 350°C prior to the arsenic capping. The InAs buffer layers were grown at 460°C on InAs(0 0 1) substrates and arsenic capped in a similar manner to the GaAs buffer layers.

After arsenic capping, the samples were removed from the MBE system and immediately remounted on Mo sample holders for a Riber 1000 MBE system and loaded into the load lock. After inserting the arsenic capped sample into the Riber 1000 growth chamber, the arsenic cap was removed by heating to 300°C for 10 min. Reflection high energy electron diffraction was used to ensure complete removal of the As-cap prior to Heusler alloy growth. The growth procedures used varied for the different Heusler alloys. For Ni_2MnGa growth on the six monolayer thick $Sc_{0.3}Er_{0.7}As$ interlayer, the sample was cooled from 300°C used for the arsenic cap removal to 200°C. Alternate layer epitaxy was used to grow five sequential monolayers of Ni and Mn+Ga to yield a Ni/Mn-Ga/Ni/Mn-Ga/Ni monolayer growth sequence at 250°C. Following this growth sequence, the sample was heated to 300°C prior to the subsequent growth of Ni_2MnGa by codeposition to a total thickness of 900 Å. The Ni_2MnGa growth rate was $\sim$0.09 μm/h. This growth procedure is similar to that described in reference [14]. The same growth procedures were used to grow Ni_2MnGe directly on GaAs without a $Sc_{0.3}Er_{0.7}As$ interlayer. For Ni_2MnIn direct codeposition on the arsenic decapped InAs(0 0 1) was done at 80°C. After the growth, the

sample was annealed at 150°C for 10 min. For all samples, a thin ~20 Å thick Al capping layer was deposited at room temperature prior to removal from the vacuum system.

3. Results and discussion

The X-ray diffraction pattern from the Ni_2MnGa (900 Å)/$Sc_{0.3}Er_{0.7}As$/GaAs(0 0 1) heterostructure shows sharp (0 0 2) and (0 0 4) diffraction peaks for both Ni_2MnGa and GaAs with the intensity of the (0 0 4) peak being greater than the (0 0 2), indicating a high quality single crystal epitaxial film. From these data, the out-of-plane lattice parameter was determined to be 6.18 Å, which is similar to that found for thinner (300 Å) pseudomorphic films [14]. The pseudomorphic growth is attributed to a new stress-induced Martensitic phase [14]. Rutherford backscattering channeling minimum yield was 6.5%, which is also indicative of an epitaxial single crystal film.

A high resolution transmission electron microscopy (TEM) micrograph of the sample is shown in Fig. 2. The abrupt six monolayer thick $Sc_{0.3}Er_{0.7}As$ layer is clearly visible. Vertical lattice fringes can also be seen in the Ni_2MnGa film. In addition, there is some contrast from layers in {1 1 2} type orientation. Although, detailed analysis has not been made, this contrast is likely to come from stress or composition variations in the film. The inset in the figure shows a convergent beam electron diffraction pattern obtained from both the GaAs and the Ni_2MnGa film. The discs in the diffraction pattern are clearly split in the vertical direction (see upper discs), while no splitting is observed in the horizontal direction. These data are consistent with the Ni_2MnGa being tetragonally distorted and pseudomorphic on the GaAs substrate. This is a surprising result and corresponds to a thickness $\geqslant$ 50 times larger than the expected critical thickness for a system with 3% mismatch. These results are supported by first principle calculations of the mechanical properties of Ni_2MnGa, which show that Ni_2MnGa has a very wide energy minimum as a function of c/a ratio [18].

Fig. 3 shows reflection high energy electron diffraction (RHEED) patterns from the Ni_2MnGe and Ni_2MnIn surfaces after growth. The 2× reconstruction

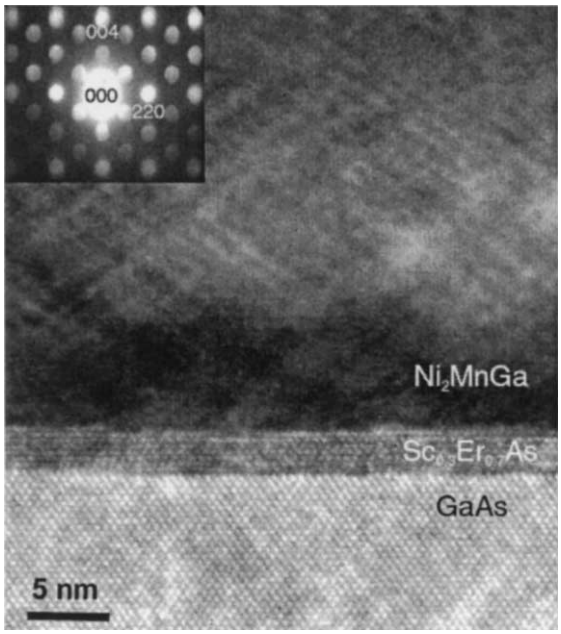

Fig. 2. Cross-sectional high resolution TEM micrograph of a $Ni_2MnGa/Sc_{0.7}Er_{0.3}As$/GaAs(0 0 1) heterostructure. The inset is a CBED pattern from the Ni_2MnGa and GaAs.

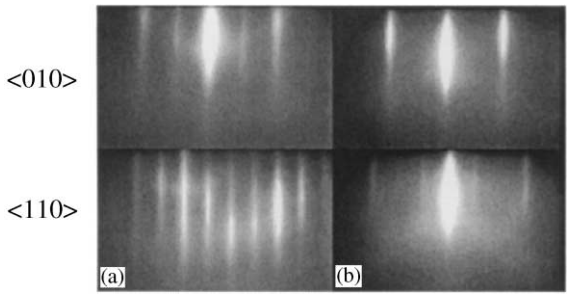

Fig. 3. RHEED patterns obtained form (a) Ni_2MnGe/GaAs (0 0 1) and (b) Ni_2MnIn/InAs(0 0 1). The top and bottom patterns were obtained with the electron beam incident along ⟨0 1 0⟩ and ⟨1 1 0⟩ directions respectively.

obtained from the Ni_2MnGe with the electron beam incident along the ⟨1 1 0⟩ and ⟨0 1 0⟩ directions of the GaAs suggest a (2×2) surface reconstruction, which is the same as that observed for Co_2MnGe [17]. X-ray diffraction data from Ni_2MnGe films show an out of plane lattice parameter of 5.896 Å, which is slightly larger than the bulk value ($a_0 = 5.70$ Å), indicating possible pseudomorphic growth. The RHEED pattern with the electron beam along ⟨1 1 0⟩ obtained from

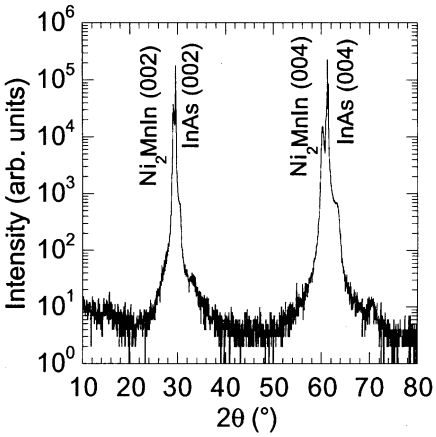

Fig. 4. X-ray diffraction θ–2θ scans of Ni_2MnIn(1000 Å)/InAs (0 0 1) structure.

the Ni_2MnIn surface (Fig. 3b) indicates that the surface unit cell is half that expected for the $L2_1$ Mn–In terminated surface with a weak $3\times$ reconstruction. The patterns would be consistent with a Ni terminated surface, a disordered Mn–In terminated surface, or a different crystal structure.

The out of plane lattice parameter determined from the diffraction scan (Fig. 4) assuming the cubic $L2_1$ structure is 6.15 Å, which, as in the case of Ni_2MnGe, is slightly larger than the bulk value (6.068 Å). However, for the $L2_1$ structure, the X-ray diffraction intensity for the (0 0 4) peak should be higher than the (0 0 2), which is not the case. This suggests that the Ni_2MnIn is growing in a different crystal structure. One possibility would be a disordered $L2_1$ structure, which would result in a CsCl structure. In this case the (0 0 2) and (0 0 4) peaks should be relabeled as (0 0 1) and (0 0 2), respectively. The lattice parameter of NiIn is 3.06 Å, which is close to half the Ni_2MnIn lattice parameter determined from Fig. 4. However, in the case of NiGa growth on GaAs(0 0 1), the hexagonal phase Ni_2Ga_3 can be grown with a pseudo cubic surface structure [19]. Hence, an alternative explanation would be the growth of an $(1\,0\,\bar{1}\,1)$ oriented hexagonal phase with the Ni_2In_3 structure and the Ni_2MnIn peaks would be identified $(1\,0\,\bar{1}\,1)$ and $(2\,0\,\bar{2}\,2)$ for the ones labeled (0 0 2) and (0 0 4) in Fig. 4, respectively. The expected planar spacing is 3.09 Å for Ni_2In_3, which is close to that observed. Further studies are required

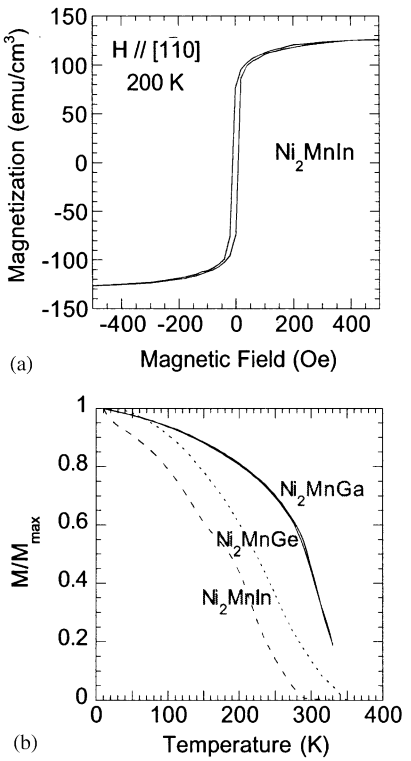

Fig. 5. (a) Magnetic hysteresis loop and (b) change in magnetization as a function of temperature.

to clarify the Ni_2MnIn crystal structure, composition and possible pseudomorphic growth on InAs.

An in-plane magnetic hysteresis loop obtained from Ni_2MnIn is shown in Fig. 5a. Similar loops were obtained from Ni_2MnGa and Ni_2MnGe. No strong in-plane anisotropy was found for the Ni_2MnGa films. Fig. 5b shows the relative magnetization versus temperature obtained using a superconducting quantum interference device magnetometer. From these data, the Curie temperatures, ~290, ~320, and ~340 K, and low temperature saturation magnetization, ~200, ~400, and ~450 emu/cm^3, were determined for Ni_2MnIn, Ni_2MnGe and Ni_2MnGa, respectively.

4. Conclusions

Heteroepitaxial ferromagnetic Ni_2MnGa/GaAs (0 0 1), Ni_2MnGe/GaAs (0 0 1), and Ni_2MnIn/InAs (0 0 1) structures have been grown by molecular beam

epitaxy. The films show in-plane magnetization with Curie temperatures close to room temperature.

Acknowledgements

This research was supported in part by Contract Nos. DARPA/ONR-N/N00014-99-1-1005, ONR-N/N00014-99-1-0233, AFOSR-F49620-98-1-0433, MRSEC Program of the National Science Foundation under Award Number DMR-9809364.

References

[1] H. Ohno, J. Magn. Magn. Mat. 200 (1999) 110.
[2] J.M. Kikkawa, D.D. Awschalom, Nature 397 (1999) 139.
[3] G.A. Prinz, Science 250 (1990) 1092.
[4] Y. Ohno, D.K. Young, B. Beschoten, F. Matsukura, H. Ohno, D.D. Awschalom, Nature 402 (1999) 790.
[5] R. Fiederling, M. Keim, G. Reuscher, W. Ossau, G. Schmidt, A. Waag, L.W. Molenkamp, Nature 402 (1999) 787.
[6] P.R. Hammer, B.R. Bennett, M.J. Yang, M. Johnson, Phys. Rev. Lett. 83 (1999) 203.
[7] A. Hirohata, Y.B. Xu, C.M. Guertler, J.A.C. Bland, J. Appl. Phys. 87 (2000) 4670.
[8] F.G. Monzon, M. Johnson, M.L. Roukes, Appl. Phys. Lett. 71 (1997) 3087.
[9] G. Schmidt, D. Ferrand, L.W. Molenkamp, A.T. Filip, B.J. van Wees, Phys. Rev. B 62 (2000) R4790.
[10] R.J.J. Soulen, J.M. Byers, M.S. Osofsky, B. Nadgorny, T. Ambrose, S.F. Cheng, P.R. Broussard, C.T. Tanaka, J. Nowak, J.S. Moodera, A. Barry, J.M.D. Coey, Science 282 (1998) 85.
[11] H.X. Tang, F.G. Monzon, R. Lifshitz, M.C. Cross, M.L. Roukes, Phys. Rev. B 61 (2000) 4437.
[12] M.W.J. Prins, H. van Kempen, H. van Leuken, R.A. de Groot, W. Van Roy, J. De Boeck, J. Phys.: C. Matter 7 (1995) 9447.
[13] K.A. Kilian, R.H. Victora, J. Appl. Phys. 87 (2000) 7064.
[14] J.W. Dong, L.C. Chen, C.J. Palmstrøm, R.D. James, S. McKernan, Appl. Phys. Lett. 75 (1999) 1443.
[15] J.W. Dong, L.C. Chen, S. McKernan, J.Q. Xie, M.T. Figus, R.D. James, C.J. Palmstrøm, Mat. Res. Soc. Symp. Proc. 604 (2000) 297.
[16] J.W. Dong, L.C. Chen, J.Q. Xie, T.A.R. Müller, D.M. Carr, C.J. Palmstrøm, S. McKernan, Q. Pan, R.D. James, J. Appl. Phys. 88 (2000) 7357.
[17] T. Ambrose, J.J. Krebs, G.A. Prinz, Appl. Phys. Lett. 76 (2000) 3280.
[18] V. Godlevsky, K.M. Rabe, Phys. Rev. B 63 (2001) 134407.
[19] A Guivarc'h, J. Caulet, B. Guenais, Y. Ballini, R. Guérin, A. Poudoulec, A. Regreny, J. Crystal Growth 95 (1989) 427.